Journal of Biomechanics 47 (2014) 1733–1738

Contents lists available at ScienceDirect

Journal of Biomechanics

journal homepage: www.elsevier.com/locate/jbiomech
www.JBiomech.com

Shoulder labral pathomechanics with rotator cuff tears

Eunjoo Hwang [a,b], James E. Carpenter [c], Richard E. Hughes [b,c,d], Mark L. Palmer [a,b,*]

[a] School of Kinesiology, University of Michigan, Ann Arbor, MI, USA
[b] Department of Biomedical Engineering, University of Michigan, Ann Arbor, MI, USA
[c] Department of Orthopaedic Surgery, University of Michigan, Ann Arbor, MI, USA
[d] Department of Industrial & Operations Engineering, University of Michigan, Ann Arbor, MI, USA

ARTICLE INFO

Article history:
Accepted 18 January 2014

Keywords:
Shoulder
Rotator cuff tears
Pathomechanics
Glenoid labrum
Long head of biceps tendon

ABSTRACT

Rotator cuff tears (RCTs), the most common injury of the shoulder, are often accompanied by tears in the superior glenoid labrum. We evaluated whether superior humeral head (HH) motion secondary to RCTs and loading of the long head of the biceps tendon (LHBT) are implicated in the development of this associated superior labral pathology. Additionally, we determined the efficacy of a finite element model (FEM) for predicting the mechanics of the labrum. The HH was oriented at 30° of glenohumeral abduction and neutral rotation with 50 N compressive force. Loads of 0 N or 22 N were applied to the LHBT. The HH was translated superiorly by 5 mm to simulate superior instability caused by RCTs. Superior displacement of the labrum was affected by translation of the HH ($P<0.0001$), position along the labrum ($P<0.0001$), and interaction between the location on the labrum and LHBT tension ($P<0.05$). The displacements predicted by the FEM were compared with mechanical tests from 6 cadaveric specimens and all were within 1 SD of the mean. A hyperelastic constitutive law for the labrum was a better predictor of labral behavior than the elastic law and insensitive to ± 1 SD variations in material properties. Peak strains were observed at the glenoid–labrum interface below the LHBT attachment consistent with the common location of labral pathology. These results suggest that pathomechanics of the shoulder secondary to RCTs (e.g., superior HH translation) and LHBT loading play significant roles in the pathologic changes seen in the superior labrum.

1. Introduction

More than 4.1 million patients present annually with symptoms related to the rotator cuff. After the third and fifth decades of life, approximately 30% and 80%, respectively, of patients will have rotator cuff tears (Duke Orthopaedics, 2013), the most common injury to shoulder joints. Tears are frequently accompanied by an associated injury to the superior glenoid labrum (Kim et al., 2003). Tears of the superior glenoid labrum are believed to cause pain and mechanical symptoms of catching and locking in the shoulder. Treatments include debridement and/or repair of the labrum and release and tenodesis of the biceps tendon.

Mechanically, the glenohumeral joint is capable of the largest range of motion in the human body. The large difference between the curvature and size of the humeral head compared with the glenoid requires both active stabilization by the rotator cuff muscles and passive stabilization by the concavity of the glenoid. The variation in cartilage thickness improves congruency between the two bones (Soslowsky et al., 1991) as does the fibrocartilaginous labrum, which increases the surface area and socket depth (Lippitt et al., 1993; Halder et al., 2001). Similar to the meniscus of the knee and the labrum of the hip, the strain experienced by the labrum correlates with susceptibility to injury. However, in situ measurements of strain in the glenoid labrum remain difficult due to the small size of the tissue and its location between the glenoid cartilage, glenoid bone, and the humeral head. The role of both active and passive factors in stabilizing the glenohumeral joint, and observations that rotator cuff tears are associated with increased superior humeral head translation (Keener et al., 2009; Mura et al., 2003; Yamaguchi et al., 2000), suggest that a causal relationship may exist between rotator cuff pathology and increased strain in the superior labrum.

In addition to its role as a passive stabilizer of the glenohumeral joint, the superior labrum is also contiguous with the origin of the long head of biceps tendon (LHBT) (Levine et al., 2000; Tuoheti et al., 2005; Vangsness et al., 1994). Increased LHBT load in activities like overhead throwing may alter glenohumeral kinematics (Youm et al., 2009) and increase strain on the labrum (Yeh et al., 2005; Rizio et al., 2007).

The effects of superior humeral head migration and LHBT tension on labral strain are not well established. Moreover, the

* Corresponding author at: University of Michigan, School of Kinesiology, 401 Washtenaw Avenue, Ann Arbor, MI 48109-2214, USA.
E-mail address: mlpalmer@umich.edu (M.L. Palmer).

0021-9290/$ - see front matter © 2014 Elsevier Ltd. All rights reserved.
http://dx.doi.org/10.1016/j.jbiomech.2014.01.036

effect of the constitutive model on the predicted mechanics of the labrum is not well understood. Previous studies that analyzed the distribution of stress and strain in the labrum used a linear, isotropic constitutive law and modeled the morphology of the labrum as a thin two-dimensional shell structure (Drury et al., 2010) or derived the three-dimensional morphology from regular geometric shapes (Yeh et al., 2005). Our previous work (Gatti et al., 2010) demonstrated the efficacy of the finite element (FE) model in predicting the displacements and strain in the labrum during humeral head translation using a linear, transversely isotropic hyperelastic constitutive law. The present study extends this work by coupling nonlinear constitutive models of the labrum with a subject-specific model of the morphology of the labrum, including the interface with and loading on the LHBT. The purpose was to analyze the interaction of labrum mechanics and cuff dysfunction by (i) validating an extended FE model with primary experimental data that includes the effects of LHBT loading, (ii) determining the effect of the constitutive model on the predicted labral response, and (iii) predicting the strain distribution within the superior labrum. We hypothesize that superior humeral head translation, as can be seen in rotator cuff disease, and LHBT loading may play a role in the development of labral pathology in patients with rotator cuff tears. The hypothesis will be supported if superior translation of the humeral head and LHBT tension causes an increase in the displacement of the superior labrum and a concomitant increase in tissue strain.

2. Materials and methods

A right shoulder with no signs of previous injury was obtained from a fresh-frozen cadaver (male, 84 years old) and dissected free of all soft tissue, except for the labrum, the LHBT origin, and the cartilages on both the glenoid and humeral head. The specimen was then scanned using a micro-CT system (GE eXplore Locus, GE Healthcare-Pre-Clinical Imaging, London, UK). Because the soft tissues were difficult to distinguish in the micro-CT images, the labrum and LHBT origin were then removed and the specimen was rescanned. A Boolean operation was then applied to the two image sets allowing segmentation and 3D reconstruction of the humeral head bone, humeral head cartilage, glenoid bone, glenoid cartilage, labrum, and the LHBT origin using Amira (Visage Imaging, Inc., San Diego, CA).

The segmented structures were converted to surface entities and smoothed before exporting them to Hypermesh (Altair Engineering, Inc., Troy, MI), an FE pre-processing tool. The bones were modeled using quadrilateral shell elements (Ellis et al., 2007). The cartilages, labrum, and LHBT origin were converted to hexahedral solid elements (Debski et al., 2005; Gatti et al., 2010; Henak et al., 2011). To simulate the clinically precise vector of the tension through the LHBT, hexahedral elements were added to the distal end of the LHBT origin by following the biceps groove. The labrum was sectioned into superior, anterior, inferior, and posterior labrum. Each labral section and the LHBT were assigned local coordinate systems to define the local fiber orientation (Gatti et al., 2010). A mesh convergence study for the glenoid, glenoid cartilage, labrum, and LHBT was performed adjusting the mesh density to ensure the numerical stability of the result. The resulting FE mesh contained 6071 solid elements, 9331 shell elements, and 16261 nodes (Fig. 1). Doubling the mesh density produced a strain difference of approximately 1% and a displacement difference of less than 1%, but caused a 10-fold increase in solution time.

Baseline material properties for each tissue were assigned based on the literature (Table 1). The bones were modeled as rigid materials because of their relatively small deformations compared to other soft tissues and the modest loading conditions in our model (Ellis et al., 2007). The cartilages were modeled as isotropic elastic materials (Huang et al., 2005; Gatti et al., 2010). The labrum was modeled as a transversely isotropic material (Quapp and Weiss, 1998), since there is a difference of approximately two orders of magnitude between the modulus in the transverse plane and the circumferential direction (Smith et al., 2008). The labrum material coefficients for the hyperelastic model were obtained by fitting the neo-Hookean constitutive equation to an experimentally derived expression for uniaxial hyperelastic behavior along the fiber direction (Weiss et al., 1996; Henak et al., 2011). Similarly, the LHBT was modeled as a transversely isotropic, hyperelastic material with an elastic modulus of 629 MPa (Carpenter et al., 2005). This modulus was chosen because it was obtained from a shoulder without rotator cuff tears at a location closer to the labrum than in other studies (McGough et al., 1996).

Boundary conditions for FE model were chosen to simulate the experimental conditions. The basic experimental protocol was published previously (Gatti et al., 2010) and was extended to include LHBT loading (Fig. 1). We positioned the humerus in 30° of abduction in the scapular plane with neutral humeral rotation. A compressive force of 50 N in the medial direction was applied to seat the humerus in the glenoid cavity (Gatti et al., 2010; Lippitt et al., 1993). Next, either 0 N or 22 N was applied to the distal end of the LHBT. A 22 N load was chosen because this load was shown to affect glenohumeral range of motion and kinematics (Gatti et al., 2010; Youm et al., 2009). Finally, the humerus was translated in the superior direction relative to the glenoid between the starting position and a peak displacement. Peak displacement ranged 1–5 mm in increments of 1 mm. The superior direction was determined by drawing a line from the center of the glenoid to the LHBT attachment (Lazarus et al., 1996). This range of displacements was used to validate the model across the spectrum of humeral head displacements that occur in healthy shoulders and ones with massive rotator cuff pathology (Mura et al., 2003). The non-sliding interfaces were modeled using tied contact. All sliding interfaces were modeled using frictionless, surface-to-surface contact due to the low coefficient of friction in synovial joints (Henak et al., 2011).

The dynamic FE analyses were performed using LS-DYNA Explicit (Livermore Software Technology Corp., Livermore, California). The predicted labral displacements were compared with data from a cadaver experiment. Since the experimental displacement was measured using plain radiographs parallel to the glenoid plane, the displacement component in the out-of-glenoid plane was not used when determining the labrum displacement from the FE analysis. The model also predicted the effective strain in the labrum as a function of the humeral head translation both with and without LHBT tension. The effective Green strain (von Mises strain) was chosen because it is a scalar quantity representing the combined

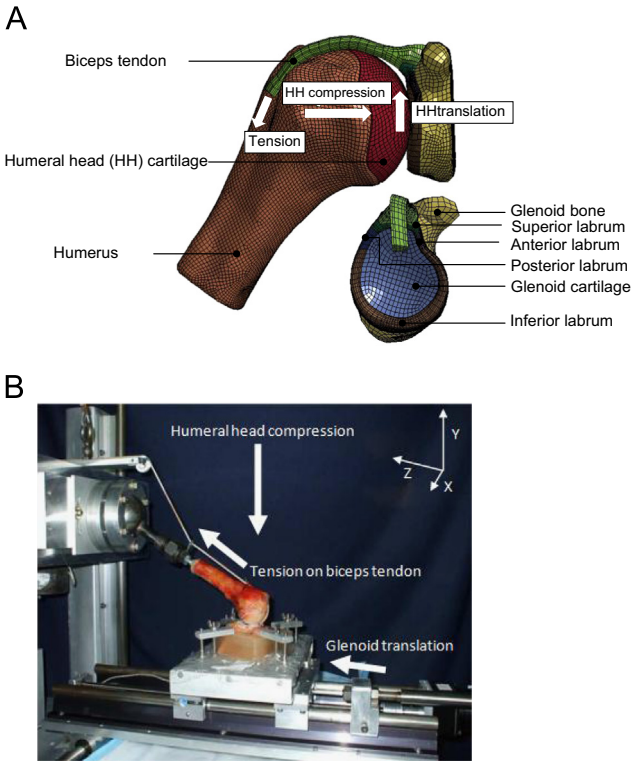

Fig. 1. (A) Three-dimensional finite element (FE) model of the glenohumeral joint, including the labrum-biceps complex. (B) Testing fixture for the validation experiment. Details of the experimental methods used to validate the model have been reported (Gatti et al., 2010). Briefly, six shoulder specimens (average 51.7 years old, range 47–55) were treated similar to the specimen for the FE model. A custom apparatus allowed motion in the superior–inferior direction of the potted scapula using an electric stepper motor. The humerus was fixed by a clamped bolt to a vertical slide using a universal joint. A 50 N load was applied through the humeral head perpendicular to the surface of the glenoid. The humerus was translated up to the maximum range of motion in each direction. Following each translation, the glenoid stage was returned to the joint center. The long head of the biceps tendon was sutured to a nylon rope, threaded through a custom eye-nut for alignment of the loading vector to the muscle's vector, and attached to a 2.2 kg weight to serve as 22 N of tensile loading. For serial radiographs, six 1-mm alloy steel beads were affixed to the labrum and five beads to the glenoid cartilage using cyanoacrylate glue. The captured radiographs were scanned and processed using ImageJ (http://rsb.info.nih.gov/ij/). The displacements of each bead were calculated according to the angular position of the labrum–glenoid bead pairs. The displacements for beads at the anterior and posterior labrum-biceps junctions were paired with the 0° glenoid bead. The inter-user reliability of the image-processing protocol was assessed and found to be robust (ICC > 0.99).